

# TOWARD AUTOMATIC BLOOD SPATTER ANALYSIS IN CRIME SCENES

A.R. Shen, G.J. Brostow, R. Cipolla

Department of Engineering, University of Cambridge, CB2 1PZ  
gjb47@cam.ac.uk  
Fax: +44-1223-332662

**Keywords:** Blood Spatter, Origin Localisation, Metrology

## Abstract

Some scenes of violent crime contain blood stains. Blood spatter stains occur when blood falls passively due to force being applied to a body. There is a well established though extremely tedious technique by which a specially trained forensic technician can analyse the individual blood spots. This procedure estimates the body's 2D location on the floorplan when the body was impacted. Our image analysis algorithm contributes an automatic and accessible alternative that could be exploited at crime scenes, assuming the stains are known to be the result of spatter. This paper presents our approach and the results of comparative experiments we used to confirm the accuracy of the algorithm.

## 1 Introduction and Background

Blood spatter analysis is performed by forensics experts at crime scenes where impact on a body has caused blood to fly off and land on surrounding surfaces. The resulting stains are affected by many physical variables, such as speed, liquid density, and the material properties of the surface. However, the shape of the stains, in this case the spatter pattern, does reveal information that can be useful to investigators. In 1895, Piotrowski [8] was the first to propose that the elongated shape and layout of the stains indicated the location of a victim's head at the time it was subjected to trauma.

Subsequent developments have led to the emergence of Blood Spatter Analysis as a forensic specialisation [4]. While great care will continue to be necessary on the part of the expert, our work proposes an image analysis technique that can automate aspects of gathering and analysing the data. Our main contribution is an algorithm that processes digital images of the crime scene to obtain the same information as the current but incredibly tedious "string method." Our secondary contribution is the exploitation of calibration objects to perform image rectification, producing shot-from-above images of the crime scene.

Blood is a complex non-Newtonian viscoelastic fluid. In contrast to Newtonian fluids, blood drops do not exhibit "wobble" after separating. While air resistance still affects the otherwise spherical shape of an airborne blood drop, such an approximation of shape is considered acceptable in

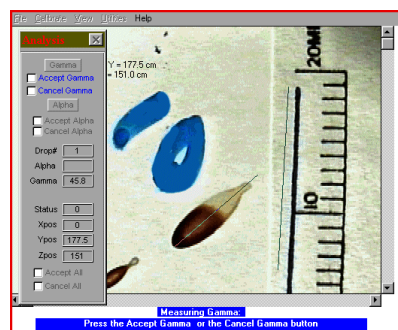


Figure 1: BackTrack™ software allows a user to click, specifying endpoints of the plumb line and points on the blood spot's major axis. Screenshot courtesy of Fred Carter, Carleton University.

practice [10]. Ideally, once the sphere lands on a flat surface, the collision flattens the liquid into an elongated shape. In reality, the collision is a complex interaction that also produces various secondary stains, but our focus is the primary stain, which is elliptical. Neglecting wind, the major axis of the ellipse indicates a ray along the drop's trajectory from its point of origin. When one physical blow generates two non-colinear stains on a flat floor, the point of convergence of the two flight directions reveals the 2D location of the blood source. If more stains are available, the localisation is overconstrained, yielding an area from which the blood likely originated. Blood from multiple impacts should produce concentrations of intersections.

The original "string method" consisted of physically pinning one end of a string at the tip of the blood stain's ellipse, and pinning the other end on the floor across the room, along the extension of the major axis. Repeating this process for up to hundreds of blood spots takes substantial time and effort, but gives the forensic expert a good idea of where the victim stood on the floorplan when hit.

The current form of the string method was developed in 1939. Beyond information about the blood's 2D travel direction, Balthazard recognised that the ratio of a stain ellipse's axes is also useful [1]. The amount of elongation relative to the width of the drop reveals the vertical impact angle,  $\alpha$ , between the blood's flightpath and the ground. The prolific blood spatter expert H.R. MacDonell later formalised this relationship as

$$\alpha = \sin^{-1} \left( \frac{W_e}{L_e} \right), \quad (1)$$

45 Degree



Figure 2: Courtesy [1]. Sequential progression of different stains that form when a blood drop collides with a flat surface. At present, only the stain produced at initial collision is considered.

where  $W_e$  and  $L_e$  are, respectively, the width and length of the primary ellipse pattern. Since the blood drop's velocity and mass are unknown, this impact angle is only used to approximate the height at which the trauma occurred; each string is still stretched straight in the direction of the major axis, but at  $\alpha$  degrees to the ground plane. Due to the projectile motion of the drops, this procedure at least places an upper bound on the height at which the victim was struck. Commercial software has been developed to compute both Equation (1) and the major axis angle,  $\gamma$ , after a user clicks points in a digital image (see Figure 1) [3, 9]. That software also allows the angles to be stored and used to graph virtual strings, to our knowledge, after each stain's global position is typed in manually. Our objective has been to automatically perform (A) the image analysis of each stain, and (B) the calibration of multiple images into an overhead picture with a unified coordinate frame. We hypothesise that computer vision could help automate and quantify the reliability of blood spatter analysis.

## 2 Approach for Individual Stains

On collision with a surface, successive bloodstains form during different phases (see Fig. 2). In the contact and collapse phase, the stain formed is the primary spatter pattern. Further non-primary spatter patterns are formed by displacement, dispersion, and retraction on the surface. The general shape of primary spatter patterns is an ellipse. Primary spatter patterns vary little between surfaces of different materials. Their shape is instead highly related to the dynamics of the blood drop before it landed.

Existing ellipse fitting techniques include linear least-squares, bias-corrected renormalisation, and other robust estimation techniques [11]. A direct least squares fitting method was used [5] because it is invariant to affine transformation of the contour with high robustness. The algorithm's Matlab implementation was adapted to have the additional functionality of area-calculations available in [6].

The image of blood spatter is the combination of primary and non-primary patterns, so ellipse fitting can be unreliable when non-primary spatter patterns dominate:

$$A_{ts} = A_{ps} \cup A_{ns}. \quad (2)$$

$A_{ts}$  is the total spatter area, while  $A_{ps}$  and  $A_{ns}$  are the primary and non-primary spatter areas, respectively. It is important to

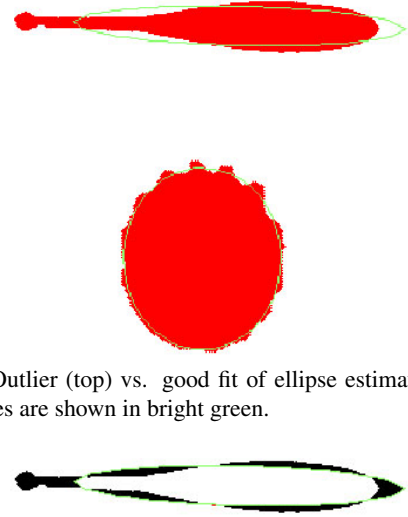


Figure 3: Outlier (top) vs. good fit of ellipse estimation (bottom), where ellipses are shown in bright green.



Figure 4: Error area computed for outlier rejection using Equation 3.

discern primary vs. secondary stains, but as impact angles get smaller, non-primary spatter patterns dominate. This makes extracting ellipse features much more difficult and inaccurate.

The presence of non-primary spatter, such as a teardrop, could falsely elongate the fitted ellipse. Therefore, such outliers must be detected and rejected, in favour of spatter stains that are closer to the origin. For this outlier rejection, an error property is defined:

$$A_{err} = \frac{A_e \cup A_{ts} - A_e \cap A_{ts}}{A_e \cap A_{ts}}, \quad (3)$$

where  $A_{err}$  is the percentage error,  $A_e$  is the fitted ellipse area, and  $A_{ts}$  is the total spatter area.

For example, in Fig. 3, the lower stain has a better ellipse fit than the upper stain because less secondary stain is present. In our quantitative outlier rejection, the upper stain will have an error area as highlighted in Fig. 4. A threshold of 90% was applied so that only the fitted ellipses that agreed with the spatter to a certain extent were kept. As a result, the estimates of  $\alpha$  had controlled deviation from the true ellipse values.

## 3 Impact Angle Experiments

The pattern of a bloodstain depends on the droplet's speed, mass, density (specifically hematocrit %), impact angle, and also the surface on which it lands. Ideally, human blood would have been used to test our algorithm, but we experimented



Figure 5: Apparatus used to collect experimental data of red liquid impacting a surface at a range of angles.

instead on paint. We are seeking collaborators who can offer real bloodstain images so we can repeat our procedure on less idealised data. In order to gather consistent images of paint spatter at various impact angles, the paint was dropped vertically onto a surface that was placed at an angle to the ground (see Figure 5). The height from which the paint was dropped influences speed, mainly changing the non-primary spatter patterns.

The surface used was plain photocopy paper. The apparatus included a clamp stand, pipette, and hardboard where paper was placed. Paint was dropped at impact angles from  $90^\circ$  to  $5^\circ$  at increments of  $5^\circ$ , and at  $20\text{cm}$  and  $40\text{cm}$  above the paper, with repetitions at each angle/height combination.

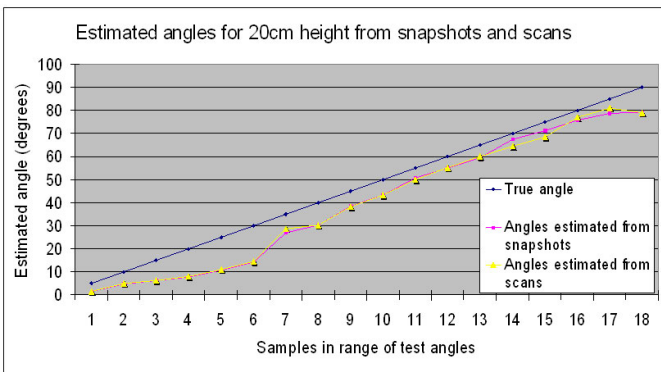


Figure 6: Graph from experiment showing the angle of impact computed using either photographed or scanned sheets of paint stains. While both are imperfect compared to the true angles, they are very close to each other, indicating that hand-held photography of blood spatter may not adversely affect our algorithm.

At small impact angles and low height, the paint tended to have displacement without dispersion. But at  $5^\circ$  impact angle and  $40\text{cm}$  above, the spatter of blood had displacement longer than the length of the paper, so only the  $20\text{cm}$  samples were made.

These paint stains were photographed digitally and also scanned on a flatbed scanner to check the reliability of handheld digital photography. The estimates of  $\alpha$  from the digital snapshots were consistent with those from the scanned

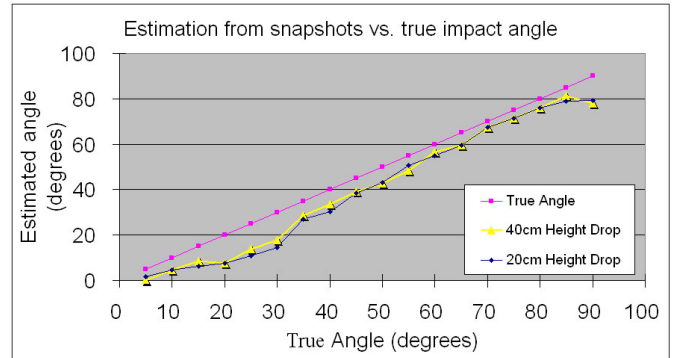


Figure 7: Graph showing actual vs. computed angles of impact, measured when dropping liquid from  $20\text{cm}$  and  $40\text{cm}$ .

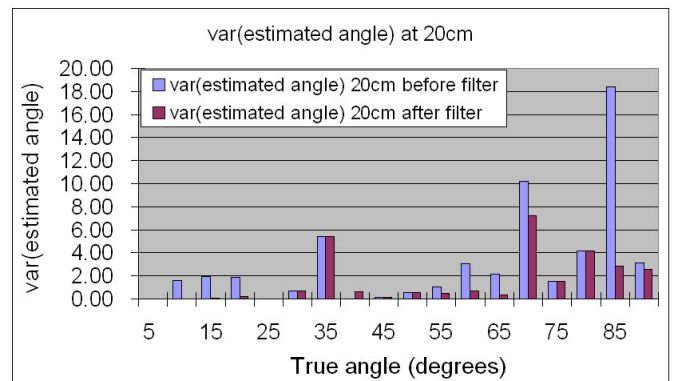


Figure 8: Absolute variance before and after outlier rejection

images (see Fig. 6). This demonstrated that careful digital photography is reliable in real applications where scanning of the crime scene is impossible.

Secondary teardrop stains form at small angles, elongating the resulting pattern. A smaller width-length ratio then results in a deflated estimate of  $\alpha$ . The first task of the algorithm is to extract the best possible primary pattern, whose contour points are used for ellipse fitting. For a paint stain that has a teardrop with a shorter tail than its primary ellipse, random sampling of data points would stay on the primary ellipse edge more than on the teardrop, therefore the least squares ellipse fitting would show a peak at the primary ellipse as desired. A more advanced sampling favoured points chosen for being further away from the major axis of the ellipse. These points had a higher chance of being on the primary ellipse rather than the teardrop. However, even this sampling breaks down when the teardrop is very long, approximately when its length exceeds 1.5 times that of the primary stain. The outlier rejection is designed to limit the impact of such situations.

The results of our experiments are plotted in Fig. 7. The estimated angles match the known angles to varying extents, but track each other as expected. There appears to be an angle-dependent bias. Interestingly, Bevel and Gardner [1] point out that it is “Difficult for a new analyst to differentiate bloodstain

lengths, particularly those in the 10 to 35 degrees range.” This suggests that an algorithm should also learn a compensatory bias. While there may be some inherent difficulty with this range of angles, we foresee using our experiment in practice, over the entire range of angles, to find the calibration that would bring the curves into alignment with the ground truth.

These results show the inclusion of outlier rejection, which was crucial in significantly reducing the absolute variance. Fig. 8 shows the negative effect of including all the spatter patterns. As the impact angles increase, the range of possible deviations from the true angle also increases, therefore, the *percentage* variance would be more appropriate when comparing the accuracy at different angles. Bevel and Gardner again give us an estimate of the accuracy one can expect from the string method: “As a general rule, the angle indicated is probably accurate to within 5 to 7 degrees.” [1] This is consistent with the results of our automatic method being applied to simulated blood.



Figure 9: Original angled view of the “crime” scene.



Figure 10: View of Figure 9’s scene rectification as if photographed from overhead.

#### 4 Application: Origin Estimation from Multiple Spots

We have established a method for estimating the direction and angle of impact of a single passive liquid drop. The main application of this method will be the localisation of the blood’s origin – the *2D* point on the floorplan of a crime scene where a body was impacted, causing the spatter. Locating the origin in *3D* is discussed in the Conclusion, but requires both the proposed algorithm and further extensions. The algorithm in Sections 2 and 3 produces a ray from each stain to an origin. To find the *2D* origin itself, one must locate the point in the plane where two or more rays converge.

The ability to capture meaningful images is an important practical consideration, with two constraints. Good ellipse fitting benefits from images where a stain is represented by a large area of pixels, photographed with the image plane parallel to the surface. But the other objective is to frame all of the crime scene’s spatter in one photograph where the rays all have the same coordinate system, and where the resulting origin can be plotted. Since CCD resolutions are increasing but are still finite, we propose that multiple photographs be registered to a common virtual image; generated to look as if the camera had been looking down at the crime scene from directly above. See the example of Figures 9 and 10.

Rectification for the task of origin-localisation requires these steps:

1. Calibrating the camera that took the original (angled) images of the crime scene,
2. Specifying a virtual overhead camera that will serve as the canonical coordinate frame,
3. Interpolation of original-pixels to synthesise the overhead picture
4. (Optional) stitching together of overlapping versions of the overhead image.

Our implementation serves as one example of how these steps can be performed. It is usually reasonable to assume that one or more visible calibration objects can be placed in the crime-scene to facilitate Steps 1 and 2. We used a checkerboard pattern in testing our prototype. We employed the camera calibration toolkit of Jean-Yves Bouguet [2] to first calibrate (off-site) a camera’s intrinsics, matrix  $K$ , using 20 images of the calibration pattern. Then, each angled photo of the scene, shot to include the calibration object, was processed to determine that view’s extrinsics,  $M_{wc}$ , the transformation from world to camera  $c$ ’s coordinates.

The interesting part of each photograph is planar, and calculating the homography allows us to view that plane, filmed with the camera at an angled position, as if it were filmed from overhead. Further details of computing a planar scene homography are in [7]. In brief, since the intrinsics

of the virtual and the several real cameras are the same, the homography between camera  $n$  and camera 1 is

$$H = KM_{wc_1}M_{wc_n}^{-1}K^{-1}. \quad (4)$$

Figures 11 and 12, and Figures 13 and 14 are examples of photographing and rectifying different parts of the same “crime scene.” The checkerboard pattern used for homography calibration serves as the common anchor for both top view rectified images. The homography transformation does not sample the original images on a regular grid, so missing pixel values are interpolated linearly. Future work can include superimposing or stitching the rectified images to render a composite visualisation that may help in court cases etc., but the canonical coordinate frame is sufficient to make combined estimates of the origin point.



Figure 11: Original *photo01*, photographed with a handheld camera viewing the blood spatter plane at an angle.

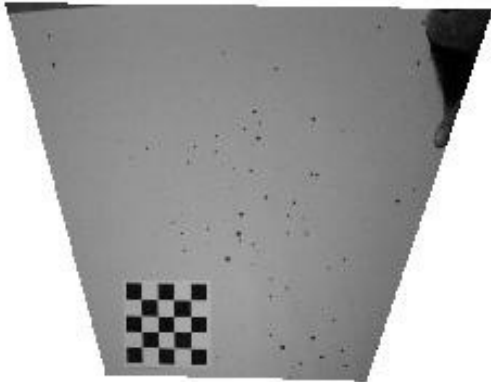


Figure 12: Version of *photo01* rectified and interpolated to appear as if photographed from directly above.

The experiment for generating the multi-spot paint stains was performed using red paint and light brown paper. A thin layer of paint was located at the top of a cylindrical container, with the liquid held together by its surface tension. A flat paddle was swung vertically onto the top of the circular container to simulate impact. The container was 22cm high and had a radius at its top of 3cm.

Fig. 15 shows the image of multiple paint stains produced by the impact. Fig. 16 shows the fitted ellipses of filtered stains

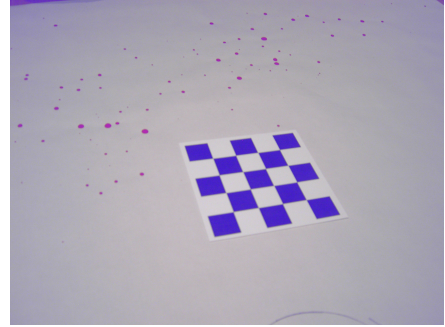


Figure 13: Color-processed *photo02*, also photographed with a handheld camera viewing the same blood spatter plane at a different arbitrary angle.

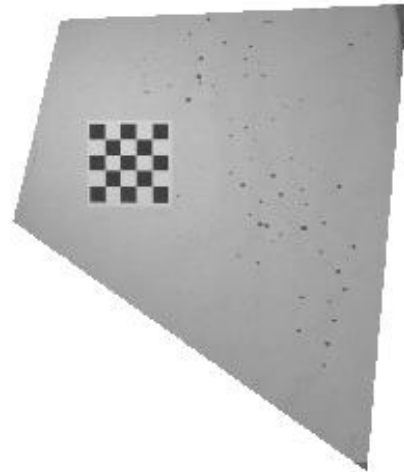


Figure 14: Version of *photo02* rectified and interpolated to appear as if photographed from directly above. Note that now, the real version of this image and Fig. 12 have compatible size and orientation to allow superimposing or stitching together into one canonical view of the scene.

and the directions estimated are drawn as straight lines. The lines cross at intercepts that represent estimates of the origin of impact.

To locate the most probable region of the origin, we generate 2D Gaussian kernels centred where pairs of rays cross. These kernels are combined additively. After normalising, this produces a height field that represents the pair-wise probability that a given 2D location is the point of origin. This constitutes a prior for RANSAC estimation, which we speculate will also reveal (in the form of multi-modal distributions) when the blood spatter is the result of multiple non-collocated impacts on the body. Running RANSAC for 500 iterations produced a map with estimated origins that was dense at the actual origin of impact area. Further testing is needed to establish the accuracy and precision of this subroutine, and to evaluate the convergence criteria of RANSAC in this case.

## 5 Conclusions and Future Work

We have demonstrated an automatic algorithm for analysis of blood spatter at crime scenes. This approach serves as



Figure 15: Rectified image of experimental multi-spot blood spatter. Note that the spatter emanated from a circular source located in the middle of the image, at the bottom edge.

an alternative to the currently employed string method. This innovation should serve to speed up the labour-intensive process of localising the blood's origin in  $2D$ . Further, it provides a quantitative metric that indicates with what certainty a given location was the source of the blood spatter. Since the experiments were performed using paint instead of blood, further trials are necessary, and these should also include non-white surfaces with various absorption properties. The experiments on paint do indicate that for single-stain analysis, the algorithm matches the accuracy expected from a forensic investigator.

Since we derived the impact angle from each fitted ellipse and the distance from each paint spot to the estimated origin, we can already roughly estimate the  $3D$  origin (height), assuming the trajectory was straight. This however, neglects the drops' projectile motion, and the many associated factors. To model the dynamics of the droplet, we could estimate its speed from its stain, to calculate the time of travel,  $t$ , and assume the initial velocity in the vertical direction was zero.

Large spatter patterns indicate the drops had more mass, which correlates approximately with slower-velocity impact to the body. The smallest spatter stains are from high-velocity impact, such as the result of gun shot wounds [10]. But significant quantities of data must be collected before this relationship can be learned, since the density of blood is not uniform. Blood is a mixture of lighter plasma proteins and heavier red blood cells (erythrocytes). These blood dynamics lead to confusion on the relationship between velocity and the size of the drops: density and aeration depend on age, fitness, alcohol and fatigue levels, and are non-uniform throughout the body (most affected by organs). Naturally, these factors are considered by forensics experts, and it is our hope that further experiments will produce a tool that is helpful to them.

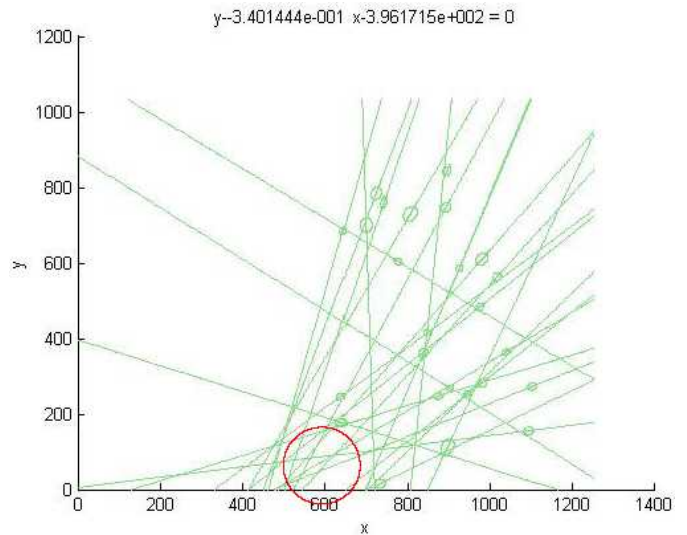


Figure 16: Result of fitting ellipses to individual liquid stains from Figure 15. While a few stains generate rays pointing away from the true blood source location, most rays cross in the correct area.

**Acknowledgements** The second author was supported by funding from the Cambridge-MIT Institute and by a Marshall Sherfield Postdoctoral Fellowship.

#### References

- [1] V. T. Bevel and R. M. Gardner. *Bloodstain Pattern Analysis: With an Introduction to Crime Scene Reconstruction*. CRC Press, 2nd edition, 2001.
- [2] Jean-Yves Bouguet. *Camera Calibration Toolbox for Matlab*. [http://www.vision.caltech.edu/bouguetj/calib\\_doc/](http://www.vision.caltech.edu/bouguetj/calib_doc/), 2004.
- [3] A.L. Carter. The directional analysis of bloodstain patterns, theory and experimental validation. *Journal of the Canadian Society of Forensic Science*, 34(4):173–189, 2001.
- [4] W. G. Eckert and S. H. James. *Interpretation of Bloodstain Evidence at Crime Scenes*. Elsevier Publishing Company, 1989.
- [5] A. W. Fitzgibbon, M. Pilu, and R. B. Fisher. Direct least squares fitting of ellipses. *IEEE Transactions on Pattern Analysis and Machine Intelligence*, 21(5):476–480, 1999.
- [6] D.C. Hanselman. Conversion from conic to conventional ellipse equation. Technical report, University of Maine, Orono, 2005.
- [7] R. I. Hartley and A. Zisserman. *Multiple View Geometry in Computer Vision*. Cambridge University Press, 2004.
- [8] Edward Piotrowski. Über entstehung, form, richtung und ausbreitung der blutspuren nach hieb- und stichwunden des kopfes. Technical report, K. K. Universität, Wien, 1895.
- [9] E.J. Podworny and A.L. Carter. Computer modeling of the trajectories of blood drops and bloodstain pattern analysis with a pc computer. In *International Association of Bloodstain Pattern Analysis News*, pages 4–12, 1990.
- [10] Anita Wonder. *Blood Dynamics*. Academic Press, 2001.
- [11] Zhengyou Zhang. Parameter estimation techniques: A tutorial with application to conic fitting. Technical Report RR-2676, Image and Vision Computing, 1997.